



# High voltage Gain DC-DC converter for Dc micro grids

Donthu. Akhil babu<sup>1</sup>, B. Ramesh<sup>2</sup>

<sup>1</sup>Department of EEE, PG Research Scholar, Sri Annamacharya Institute of Technology and Science, rajampet, Y.S.R Kadapa, A.P,

<sup>2</sup>Department of EEE, Professor, Sri Annamacharya Institute of Technology and Science, rajampet, Y.S.R Kadapa, A.P,

**ABSTRACT:** DC Micro Grids powered by solar photovoltaic systems are often made of plentiful, clean, and non-polluting renewable or non-conventional energy sources. In order to provide the necessary output power levels for residential loads, the article constructs a solar photovoltaic system-driven DC Micro Grid using high voltage gain non-isolated DC-DC converters. The suggested Modified SEPIC Converter (MSC), although similar to the typical or traditional SEPIC converter, provides the DC micro grids with continuous current and a greater voltage gain. Additionally, there is just one controlled switch needed to run this MSC. To efficiently meet the criteria for DC loads, MSC with PV system-based DC micro grids is built here. Additionally, the whole work is done using MATLAB/SIMULINK software.

**KEYWORDS:** Modified SEPIC converter, Single controlled switch, Photovoltaic systems and DC Micro Grids

## 1. INTRODUCTION

Fuels and other non-renewable energy sources were formerly used to power utility systems. However, as time goes on and people use fossil fuels more and more to satisfy their needs in the transportation and electrical energy sectors, those resources are depleting [1]. Here, the issue is that the use of conventional or non-renewable energy sources, such coal, nuclear power, and the like, is causing the air to fill with dangerous gasses like SO<sub>2</sub>, CO, and CO<sub>2</sub>. Air pollution and the greenhouse impact on the environment are mostly caused by high levels of CO<sub>2</sub> gasses in the atmosphere [2]. A Sinopec pipeline explosion occurred in China's Shandong Area in 2013, resulting in the deaths of 55 persons. These extreme blackmails are the responsibility of the coal and oil companies. Thus, administration leaders are concentrating on alternate energy sources in order to prevent these serious hiccups [3].

All scholars are now looking on alternative energy sources as a means of providing electricity without contributing to air pollution, global warming, or other issues. According to the study, alternative energy sources are those that provide electrical energy to fulfill load demand without accelerating any hazardous gasses, such as renewable or non-conventional energy sources. Because they are readily available in the environment, solar and wind energy sources are the primary non-conventional energy sources for the (DG) Distributed Energy systems. Other non-conventional energy sources include biomass sources, geothermal energy, and other resources found in certain environments [4]. However, solar and wind energy sources are accessible in all geographical areas and are freely and cleanly available in the environment [5]. Generally speaking, when combined with other renewable energy sources, solar and wind energy provide the highest efficiency. Additionally, the organization of these two non-conventional energy domains to the DC and AC Grids is the focus of all study [6].

The DC Micro Grid's general layout for DC loads using unconventional energy sources (such as wind, photovoltaic, and others) is shown in Figure 1. The DC Micro Grids' integration with unconventional energy sources allows for the precise allocation of DC power to the DC loads. Therefore, the use of DC loads in DC Micro Grids that are managed by non-isolated DC-DC converters is the focus of this research project. Thus, solar systems are selected as DC Micro Grid input sources. In general, solar photovoltaic systems use sunshine to create electricity directly. They need little area, cheap cost, and optimal efficiency when used in conjunction with solar thermal collectors. As a result, research is being done on DC Micro Grids to meet the DC load demands of solar photovoltaic systems. Low voltage stress between switches and diodes is how non-isolated DC-DC converters are controlled in [7–20].

Low voltage stress across switching techniques was previously recognized to reduce the overall system cost and switching loss. Small component stresses, a broad regulation series, negligible output ripple, good efficiency, and flexible gain extension characterize these

converters. These converters nonetheless have weak control and pulsing current while achieving high gain. Two switches are used to operate this converter; these switches also exert effort on the controller structure and disrupt utility side efficiency. In order to address the issues with the non-isolated and isolated DC-DC converters discussed in [7]–[20], MSC [21] are suggested. Since HBC and MSC include resonant components, such as passive parts across the switch to eliminate undesired disturbances and switch stress, MSC cannot produce any voltage ripples even if these converters take DC voltage with certain modifications [22]. When it comes to supply sources, MSC uses them a great deal. In order to provide DC Micro Grids with continuous output current and high voltage gain for the DC loads, MSC are used as DC-DC converters in solar system-based DC Micro Grids.

Organizing the remaining paper in this manner: Section 2 addresses the MSC's operational mechanism. The modeling results of the PV system-based DC micro grid with MSC are explained in Section 3. Additionally, MATLAB/SIMULINK software is used to do all of the simulation results. This paper is concluded in Section 4.

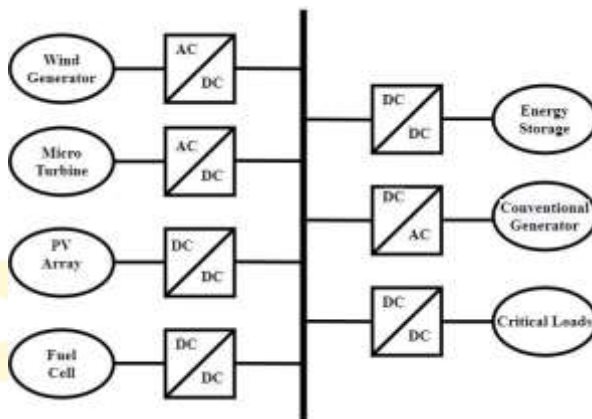


Fig.1 Overview of DC Micro Grid

## 2. PROPOSED MODIFIED SEPIC CONVERTER

The non-isolated Modified SEPIC Converter (MSC) is realized for HV applications. MSC containing the single input-output terminals and derived through shifting a conventional SEPIC converter with boost up mode as viewed in Figure 3 demonstrate the circuit diagram of the MSC containing inductors ( $L_x$ ,  $L_y$  and  $L_z$ ) are three, diodes ( $D_x$ ,  $D_y$ , and  $D_z$ ) are three, and capacitors ( $C_x$ ,  $C_y$ , and  $C_z$ ) are three, these components are controlled with a single switch  $S$  with switching frequency ( $f_s$ ). The capacitor  $C_x$  and inductor  $L_y$  attend as the voltage-boosting arrangement in adding with  $D_x$ ,  $D_y$  diodes in MSC. To assess the steady-state process of the MSC succeeding conventions are deliberated by all components in the MSC reflected as presence model and all capacitors in MSC are large and necessarily to achieve constant DC voltage. The MSC can operate in two modes as mode-1 and mode-2 as exposed in Fig.3.a and 3.b individually to fetch the continuous current at load side.

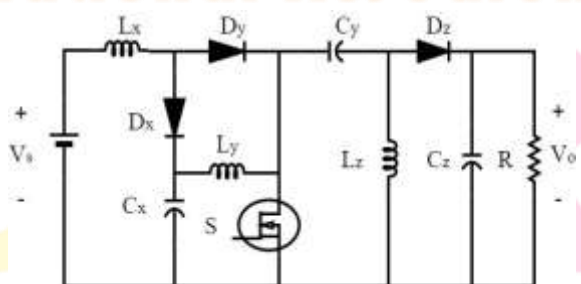


Fig. 2 Circuit diagram of a Modified SEPIC Converter

(ii). Mode-1 [ $t_0 - t_1$ ]:

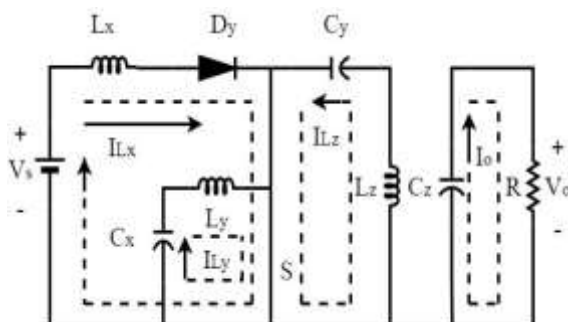


Fig. 3.a Equivalent Circuit diagram of MSC in mode-1

In mode-1, 3 inductors are reaching the subsequent current path once these inductors are magnetized: inductor  $L_x$  from input voltage ( $V_s - V_{Lx} - D_x - S - V_s$ ), inductor  $L_y$  from capacitor  $C_x$  ( $V_{Cx} - V_{Ly} - S - V_{Cx}$ ), and inductor  $L_3$  from capacitor  $C_y$  ( $V_{Cy} - S - V_{Lz} - V_{Cy}$ ). On this instant diode,  $D_z$  is reverse biased by capacitor  $C_z$  and transferral the energy to the DC load as visible in Figure 4.a.

$$V_{Lx} = V_s \quad \dots\dots\dots (1)$$

$$V_{Ly} = V_{Cx} \quad \dots\dots\dots (2)$$

$$V_{Lz} = V_{Cy} \quad \dots\dots\dots (3)$$

In mode-1, Here  $V_{Cx}$ ,  $V_{Cy}$  is the voltage across capacitor  $C_x$ ,  $C_y$  individually.  $V_{Lx}$ ,  $V_{Ly}$ ,  $V_{Lz}$  are the voltages across inductor  $L_x$ ,  $L_y$ ,  $L_z$  individually. And also in mode-1, voltage across the inductor ( $V_{Lx}$ ) is equal to supply voltage ( $V_s$ ), voltage across the inductor ( $V_{Ly}$ ) is equal to voltage across the capacitor ( $V_{Cx}$ ), and voltage across the inductor ( $V_{Lz}$ ) is equal to voltage across the capacitor ( $V_{Cy}$ ). From equation-(1), it is concluded that, the supply current coming from the input source is exactly equal to the current passing through the inductor ( $I_{Lx}$ ) This feature aids for MSC for continuous current generation at supply side. The capacitors  $C_x$ ,  $C_y$ , and  $C_z$  are charged by utilizing inductor currents  $I_{Lx}$ ,  $I_{Ly}$ , and  $I_{Lz}$  in mode-1.

(ii). Mode-2 [ $t_1 - t_2$ ]:

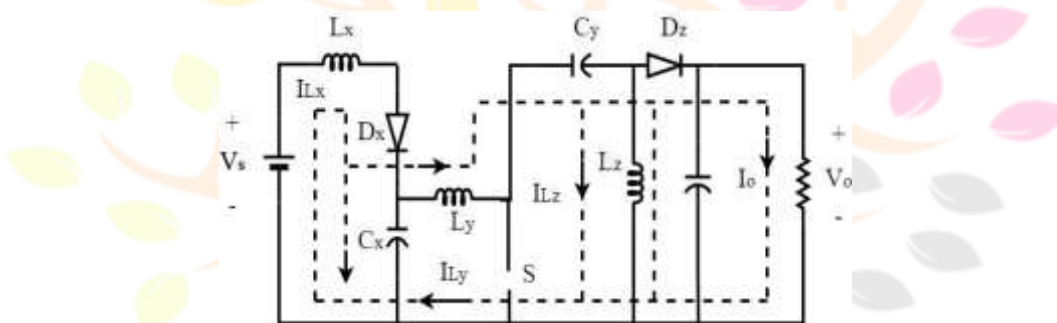


Fig.3.b Equivalent Circuit diagram of MSC in mode-2

In mode-2, 3 inductors are reached subsequent current path after these inductors are magnetized:  $L_x$  with input voltage ( $V_s$ ) charges the  $C_x$  as ( $V_s - V_{Lx} - D_x - C_x - V_s$ ). The arrangement of  $L_y$  and  $C_x$  charges to capacitor  $C_y$  as in path ( $V_{Cx} - V_{Ly} - V_{Cy} - D_z - V_o - V_{Cx}$ ). Also on this instant, inductor  $L_z$  discharges over the DC load with the path ( $V_{Lz} - D_z - V_o$ ) as visible in Figure 4.b.

$$V_{Lx} = V_s - V_{Cx} \quad \dots\dots\dots (4)$$

$$V_{Ly} = V_s - V_{Lx} - V_{Cy} - V_o \quad \dots\dots\dots (5)$$

$$V_{Ly} = V_{Cx} - V_{Cy} - V_o \quad \dots\dots\dots (6)$$

$$V_{Lz} = V_o \quad \dots\dots\dots (7)$$

In mode-2, whatever the voltage available at loads side ( $V_o$ ) is equal to the voltage across the inductor ( $V_{Lz}$ ). This feature aids the continuous voltage at load side for constant DC voltage loads. Here current passing through the inductor ( $I_{Ly}$ ) utilizes two paths deliberated in equations-(5) and (6) to produce voltage across the inductor ( $V_{Ly}$ ) without ripple content. But in mode-2, voltage across the inductor ( $V_{Lx}$ ) is equal to the difference in voltages of supply voltage ( $V_s$ ) and capacitor voltage ( $V_{Cx}$ ). The capacitors  $C_x$ ,  $C_y$ , and  $C_z$  are discharged by utilizing inductor currents  $I_{Lx}$ ,  $I_{Ly}$ , and  $I_{Lz}$  in mode-2.

By using the voltage-second balancing equation for the equations of (1) to (7), the equations (8) to (10) are concluded and these (8) to (10) equations are forms the equation of voltage gain for the MSC in equation-(11).

$$\frac{V_{Cx}}{V_s} = \frac{1}{1 - k} \quad \dots\dots\dots (8)$$

$$V_{Cy} = \frac{V_{Cx}}{1 - k} - V_o \quad \dots\dots\dots (9)$$

$$\frac{V_o}{V_{Cx}} = \frac{k}{1 - k} \quad \dots\dots\dots (10)$$

$$M_{ccm} = \frac{V_o}{V_S k} \quad \dots\dots\dots (11)$$

$$= \frac{1}{(1 - k)^2}$$

The passive elements like capacitors (C), Inductors (L), diodes (D),  $V_{ds}$ , is the voltage across the diode,  $V_{cs}$  is the voltage across the switch (S) and voltage gain ( $M_{ccm}$ ) of MSC. Voltage gain and Voltages across the switch of MSC are best suits for the High voltage applications.

### 3. RESULTS AND DISCUSSIONS

#### 3.1 SIMULATION CIRCUIT DIAGRAM OF THE MSC:

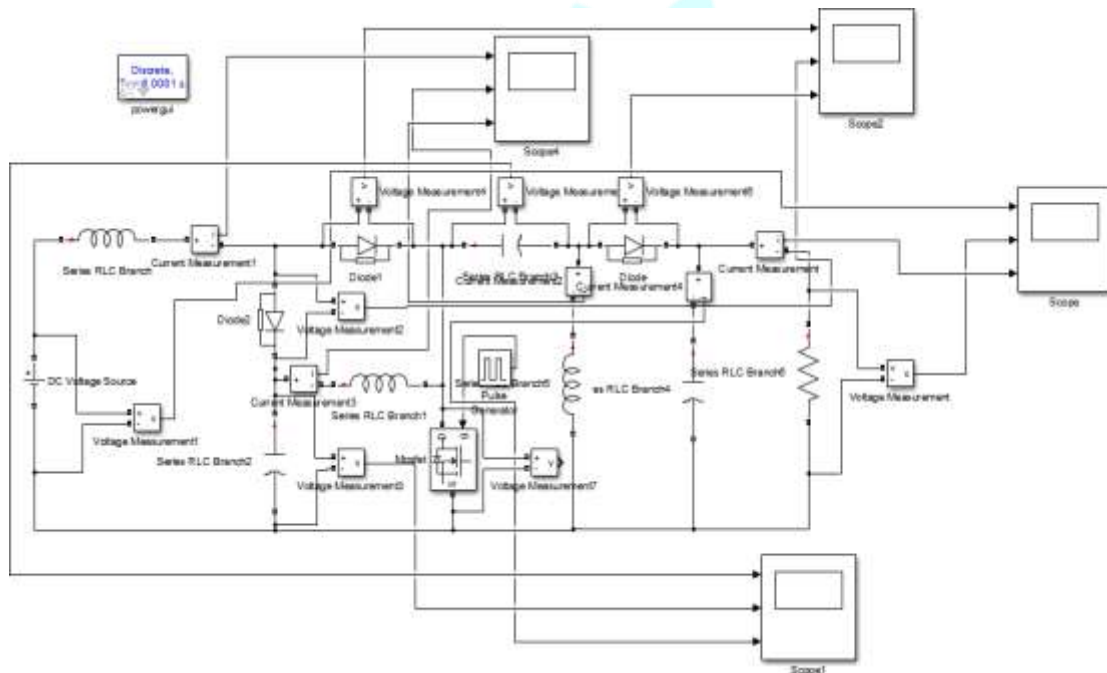


Fig.4 Simulation Circuit Diagram of the MSC

Figure 4.1's MSC simulation circuit depicts the fundamental boost module of a traditional SEPIC converter. Here,  $C_x$ ,  $L_y$  serve as resonating components for the power switch S. With the aid of these resonating elements, any switching stress and switching power losses pertaining to this switch S may be decreased. Thus, one of this circuit diagram's most notable features is its ability to generate a large voltage gain while maintaining a constant output current. Additionally, this MSC always makes the best use of its resources. Then, MSC is commonly used to achieve voltage gain more effectively. The variable duty ratio approach is a commonly used PWM technique to efficiently supply a gate voltage to the power switch, and this MSC is typically run at a set frequency. Thus, the MATLAB/SIMULINK program successfully simulates this MSC and generates an output voltage at a higher voltage gain with the requested output current needed by the DC load for DC micro grids applications.

#### 3.2 SIMULATION RESULTS OF THE MSC:

The variable duty ratio approach is a commonly used PWM technique to efficiently supply a gate voltage to the power switch, and this MSC is typically run at a set frequency. Thus, the MATLAB/SIMULINK program successfully simulates this MSC and generates an output voltage at a higher voltage gain with the requested output current needed by the DC load. Thus, DC micro grids and PV system applications are good fits for this MSC. Conventional non-isolated DC-DC converters, however, result in ripples that range from 0.1% to 0.5%. However, MSC generates ripple content at a rate of around 0.016. This voltage ripple is really small. Because of this, the output voltage and current of this converter are produced efficiently and without any ripples.

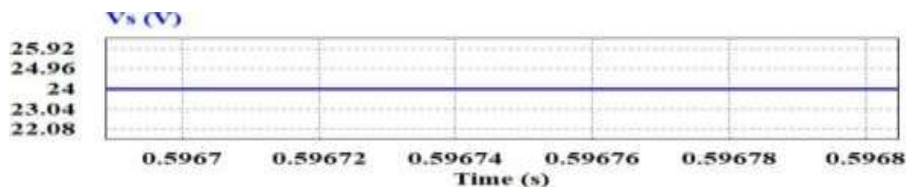


Fig.4.1 DC supply voltage  $V_s$

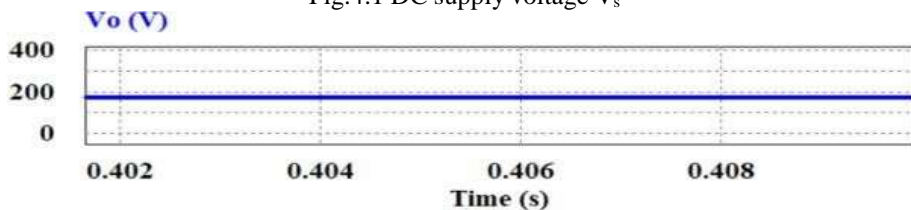


Fig.4.2 DC output voltage  $V_o$

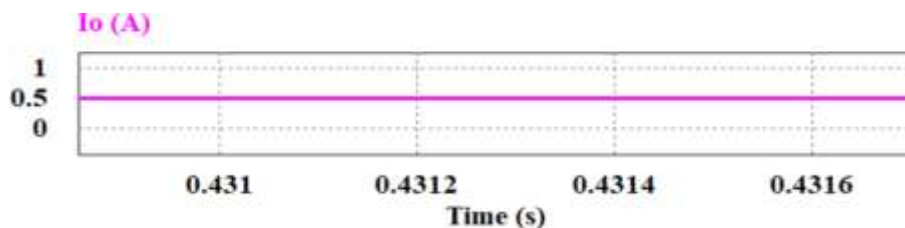


Fig.4.3 DC output current  $I_o$

The supply voltage, output voltage, and output current simulation result waveforms of the MSC with values of 24V, 186.3V, and 0.5A are shown in figures 4.1 to 4.3. The nature of these three waveforms is periodic DC. In this case, MSC is unable to produce any output voltage or current ripples. For this reason, the MSC continuously generates current for the DC loads. The simulation result waveforms of the inductor  $L_x$ ,  $L_y$ , and  $L_z$  current with respect to the MSC are shown in figures 4.4 to 4.6. The average current values are 4.2 A, 1.4 A, and 0.5 A. Three inductors' currents are growing with a positive slope in mode-I operation, and vice versa in mode-II. The simulation results for capacitor voltages VC1 and VC2, with values of 78.71V and 76.75V, are shown in figures 4.7 and 4.8. It is investigated and found that the voltage across capacitors C1 and C2 is around +80 V. The characteristic waveforms and the simulation results of the capacitor voltages VC1 and VC2 are studied, and it is shown that they are both steady state in nature. Peak Inverse Voltages of 76V and 184V are produced by these diodes, which are comparable to the values of the capacitors  $C_x$  and  $C_z$ . When in mode II, diode  $D_y$  is in reverse bias and produces a peak inverse voltage of 186.3V, which is equal to the output voltage ( $V_o$ ).

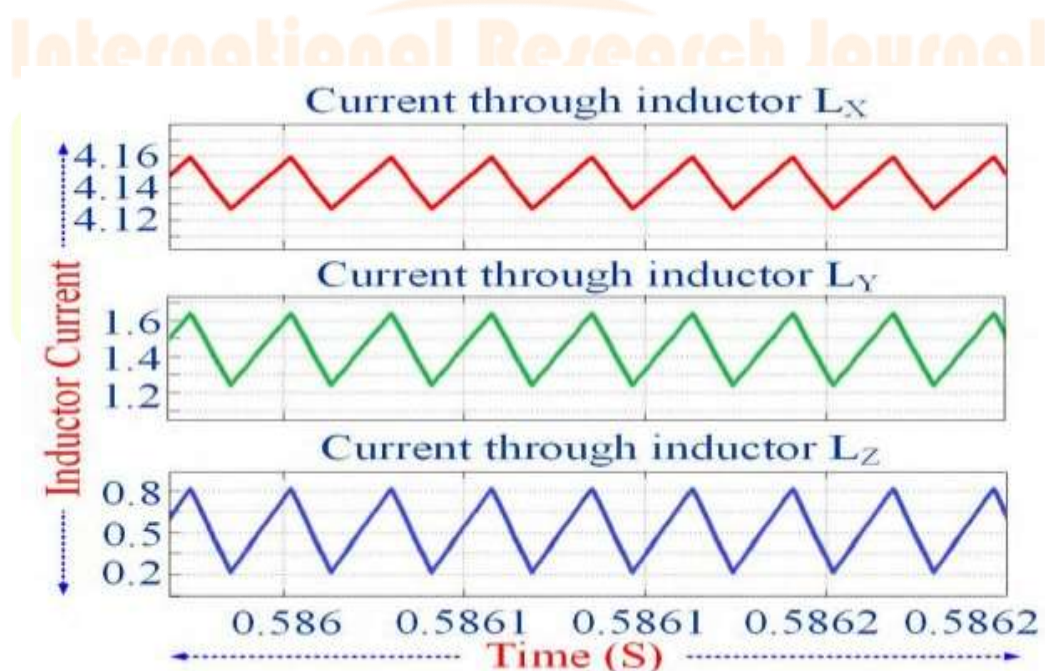


Fig.4.4-4.6 Inductor currents  $I_{Lx}$ ,  $I_{Ly}$  and  $I_{Lz}$

Usually, a constant frequency and variable duty cycle approach is used by this MSC to efficiently provide a gate voltage for the switch. As a result, MATLAB/SIMULINK software effectively simulates this MSC and generates voltage at the load side with improved voltage gain. This converter's selected output current is crucial for the DC loads in DC MicroGrids. Here, MSC findings are

obtained using MATLAB/SIMULINK for both constant and variable DC supply sources without producing ripple content in the output voltage or current.

Thus, DC MicroGrids and high voltage PV systems may use this MSC. The simulation result waveform of the current flowing in the capacitor  $C_z$  with a value of 0.5A [average value] is shown in figure 4.9. This capacitor's average current precisely matches the output current passing via resistor R. The diodes  $D_x$ ,  $D_y$ , and  $D_z$  blocking voltages under reverse bias conditions are shown in figures 4.10 through 4.12. Diodes  $D_x$  and  $D_z$  are in a forward bias state during mode I.

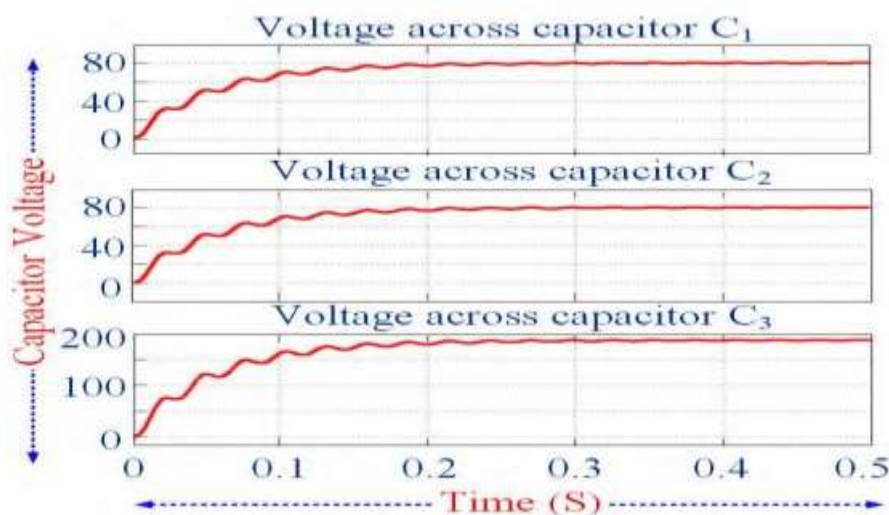


Fig.4.7-4.9 Capacitor voltage  $V_{C1}$ ,  $V_{C2}$  and  $V_{C3}$

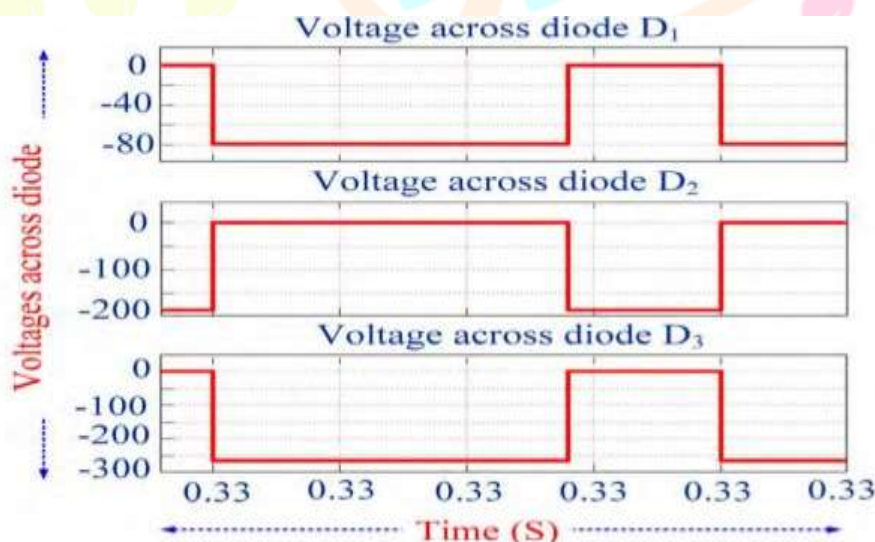


Fig.4.10-4.12 Diode voltage  $V_{D1}$ ,  $V_{D2}$  and  $V_{D3}$

Table.1 Evaluation of the simulation results of the MSC

Parameters	Values
Supply voltage $V_s$	24V
Output voltage $V_o$	186.3V
Output current $I_o$	0.5A
Inductor currents $I_{Lx}$ , $I_{Ly}$ , $I_{Lz}$	4.2A,1.4A,0.5A
Capacitor voltages $V_{C1}, V_{C2}$	78.71V,76.75V

$I_{C3}$ Current flowing in the capacitor $C_3$	0.5A
Diode Peak Inverse Voltages $I_{D1}, I_{D2}, I_{D3}$	76V,172V,184V
Voltage gain $M_{ccm}$	7.7

### CONCLUSION

The MSC can successfully meet the DC load requirement by producing continuous current, steady DC voltage without any ripples, and high efficiency at 0.7 duty ratio, according to the simulation findings for photovoltaic based DC micro grids. Additionally, the suggested MSC topology has the unique ability to reverse the supply-side current ripple when the duty cycle exceeds 0.5. The MSC's property of a high voltage gain with maximal input resource usage is accumulated.

### REFERENCES:

- [1] F. Blaabjerg, Y. Yang, K. Ma, and X. Wang, Power electronics—"The key technology for renewable energy system integration," in Proc. Int. Conf. Renew. Energy Res. Appl. (ICRERA), Nov. 2015, pp. 1618–1626.
- [2] N. Eghtedarpour and E. Farjah, "Distributed charge/discharge control of energy storages in a renewable-energy-based DC micro-grid," IET Renew. Power Gen., January 2014, vol. 8, no. 1, pp. 45–57.
- [3] Wikipedia. "Fossilfuels vs. renewable energy resources," [Online]. Available at <http://www.ecology.com/2011/09/06/fossil-fuels-renewable-energy-resources/>.
- [4] J. Hofer, B. Svetozarevic, and A. Schlueter, "Hybrid AC/DC building microgrid for solar PHOTOVOLTAIC and battery storage integration," International Conference on DC micro grids, 2017, doi: 10.1109/ICDCM.2017.8001042.
- [5] D. Kumar, F. Zare, and A. Ghosh, "Dc micro grid technology: System architectures, ac grid interfaces, grounding schemes, power quality, communication networks, applications, and standardizations aspects," IEEE Access, 2017, vol. 5, pp. 12 230–12 256.
- [6] R. W. Erickson and D. Maksimovic, "Fundamentals of Power Electronics", 2nd ed. Norwell, MA, USA: Kluwer, 2001.
- [7] M. Nymand and M. A. E. Andersen, "High-efficiency isolated boost DC–DC converter for high-power low-voltage fuel-cell applications," IEEE Trans. Ind. Electron., 2014, vol. 57, no. 2, pp. 505–514.
- [8] K. I. Hwu and W. Z. Jiang, "Isolated step-up converter based on fly back converter and charge pumps," IET Power Electron., 2014, vol. 7, no. 9, pp. 2250–2257.
- [9] Lin, B.R., Hsieh, F.Y., Chen, J.J.: 'Analysis and implementation of a bidirectional converter with high converter ratio'. IEEE Int. Conf. Industrial Technology (ICIT'08), 2008, pp. 1–6.
- [10] M. Lakshmi and S. Hemamalini, "Non-isolated high gain DC–DC converter for DC MicroGrids," IEEE Trans. Ind. Electron., vol. 65, 2018, no. 2, pp. 1205–1212.
- [11] W. Li and X. He, "Review of non-isolated high-step-up DC/DC converters in photovoltaic Grid-connected applications," IEEE Trans. Ind. Electron., vol. 58, 2011, no. 4, pp. 1239–1250.
- [12] Y. Cao, V. Samavatian, K. Kaskani, and H. Eshraghi, "A novel non-isolated ultra-high-voltage-gain DC–DC converter with low voltage stress," IEEE Trans. Ind. Electron., 2017, vol. 64, no. 4, pp. 2809–2819.
- [13] D. Yu, J. Yang, R. Xu, Z. Xia, H.-H. C. Iu, and T. Fernando, "A family of module-integrated high step-up converters with dual coupled inductors," IEEE Access, 2017, vol. 6, pp. 16256–16266.
- [14] M. Zhang, Y. Xing, H. Wu, H. Hu, and X. Ma, "A dual coupled inductors based high step-up/step-down bidirectional DC-DC converter for energy storage system," in Proc. IEEE Appl. Power Electron. Conf. Expo. (APEC), Tampa, FL, USA, Mar. 2017, pp. 2958–2963.
- [15] M. Nilanjan and S. Dani, "Control of cascaded DC–DC converter-based hybrid battery energy storage systems—Part I: Stability issue," IEEE Trans. Ind. Electron., 2016, vol. 63, no. 4, pp. 2340–2349.
- [16] J. C. Rosas-Caro, F. Mancilla-David, J. C. Mayo-Maldonado, J. M. Gonzalez-Lopez, H. L. Torres-Espinosa, and J. E. Valdez-Resendiz, "A transformer-less high-gain boost converter with input current ripple cancelation at a selectable duty cycle," IEEE Trans. Ind. Electron., 2013, vol. 60, no. 10, pp. 4492–4499.
- [17] Y. Tang, T. Wang, and Y. He, "A switched-capacitor-based active-network converter with high voltage gain," IEEE Trans. Power Electron., 2014, vol. 29, no. 6, pp. 2959–2968.
- [18] Soedibyo, B. Amri and M. Ashari, "The comparative study of Buckboost, Cuk, Sepic and Zeta converters for maximum power point tracking photovoltaic using P&O method," 2nd International Conference on Information Technology, Computer, and Electrical Engineering (ICITACEE), Semarang, 2015, pp. 327–332.
- [19] K.H. Beena, Anish Benny, "Analysis and Implementation of Quadratic Boost Converter for NanoGrid Applications," International Journal of Advanced Research in Electrical, Electronics and Instrumentation Engineering (IJAREEIE), Vol. 4, Issue 7, July 2015, DOI: 10.15662/ijareeie.2015.0407030 6043.
- [20] B. Wu, S. Li, Y. Liu, and K. M. Smedley, "A new hybrid boosting converter for renewable energy applications," IEEE Trans. Power Electron., 2016, vol. 31, no. 2, pp. 1203–1215.
- [21] Pandav Kiran Maroti, Sanjeevikumar, Padmanaban Jens Bo Holm-Nielsen, Mahajan Sagar Bhaskar, Mohammad Meraj, and Atif Iqbal, "A New Structure of High Voltage Gain SEPIC Converter for Renewable Energy Applications," IEEE Access, Vol. 7, July 2019, doi: 10.1109/ACCESS.2019.29255.

Biography of authors:

Author 1:



**Donthu. Akhil babu**, he was a PG Research Scholar in Sri Annamacharya Institute of Technology and Science, rajampet, Y.S.R Kadapa, A.P. His was interested in power electronics and drives, electrical machines and renewable energy sources.

Author 2:



**B.Ramesh**, he was a working as a professor in Sri Annamacharya Institute of Technology and Science, rajampet, Y.S.R Kadapa, A.P. His current is power electronics and drives, electrical machines and renewable energy sources.

International Research Journal  
**IJNRD**  
Research Through Innovation